Microelectronics Reliability 55 (2015) 1427–1432

Contents lists available at ScienceDirect

Microelectronics Reliability

journal homepage: www.elsevier.com/locate/mr

Comparison of analytic distribution function models for hot-carrier degradation modeling in nLDMOSFETs

P. Sharma [a,*], S. Tyaginov [a,b], Y. Wimmer [a], F. Rudolf [a], K. Rupp [a], H. Enichlmair [c], J.-M. Park [c], H. Ceric [a], T. Grasser [a]

[a] Institute for Microelectronics, Technische Universität Wien, 1040 Wien, Austria
[b] Ioffe Physical–Technical Institute, Russian Academy of Sciences, St. Petersburg 194021, Russia
[c] ams AG, Unterpremstätten, Austria

ARTICLE INFO

Article history:
Received 28 May 2015
Received in revised form 19 June 2015
Accepted 20 June 2015
Available online 28 June 2015

Keywords:
Distribution function
Hot-carrier degradation
nLDMOS transistor
Spherical harmonics expansion
Drift–diffusion scheme
Interface states
Modeling

ABSTRACT

We analyze the applicability of different analytic models for the carrier distribution function (DF), namely the heated Maxwellian, the Cassi model, the Hasnat approach, the Reggiani model, and our own concept, to describe hot-carrier degradation (HCD) in nLDMOS devices. As a reference, we also obtain the carrier distribution function as a direct solution of the Boltzmann transport equation using the spherical harmonics expansion method. The DFs evaluated with these models are used to simulate the interface state generation rates, the interface state density profiles, and changes of the linear and saturation drain currents as well as the threshold voltage shift. We show that the heated Maxwellian approach leads to an underestimated HCD at long stress times. This trend is also typical for the Cassi and Hasnat models but in these models HCD is underestimated in the entire stress time window. While the Reggiani model gives good results in the channel and drift regions, it cannot properly represent the high-energy tails of the DF near the drain, and thus leads to a weaker curvature of the degradation traces. We show finally that our model is capable of capturing DFs with very good accuracy and, as a result, the change of the device characteristics with stress time.

1. Introduction

A physics-based model for hot-carrier degradation (HCD) needs to be based on a microscopic description of Si–H bond-breakage mechanisms [1–4]. As has been already established, both the single- and multiple carrier processes contribute to defect generation [1,5,6]. A solitary hot carrier can induce a bond-breakage event in a single collision, which is called a single-carrier process. If the carrier flux is substantial but carriers have low energies, several cold carriers subsequently interacting with the bond can heat and eventually rupture it. Such a scenario corresponds to the multiple-carrier process. The rates of these processes are determined by the carrier energy distribution function (DF) which determines the probability density to find a carrier in a certain elementary energy range. A rigorous way to obtain the carrier distribution functions is to solve the Boltzmann transport equation (BTE). There are two different strategies to achieve this goal: the stochastic Monte-Carlo method [7,8] and the deterministic approach based on the spherical harmonics expansion (SHE). In the former method one needs to consider the trajectories of each carrier (from a representative particle ensemble) in the multidimensional space. As a result, computational resources needed for this task become cumbersome. An alternative approach is to represent the DFs as a series of spherical harmonics [9]. As opposed to the Monte Carlo method, this approach relies on a substantial amount of memory (required to store all the variables) rather than on CPU power. However, even this deterministic SHE method has high computational demands.

As such, it would be highly attractive if the solution of the BTE could be replaced by a simplified approach which represents the DF by an analytic expression. There are many different models/concepts which could be employed in the context of HCD: the heated Maxwellian distribution [10], the Cassi model [11], the Hasnat model [12], the Reggiani model [2,13], and our own approach [14]. In this work, we analyze the applicability of these models in the context of HCD in nLDMOS devices. As a reference, we also obtain the carrier distribution from our deterministic Boltzmann transport equation solver ViennaSHE [15]. The DFs obtained from the different models are used in our HCD model to predict the degradation in nLDMOS devices. These degradation curves are compared with the experimental data and a conclusion on the validity of each model is drawn. Since all models use the same parameter set, the differences in the results can be directly traced back to inaccuracies in the approximation of the DF.

2. The devices and stress conditions

We performed hot-carrier stresses on nLDMOS transistors (sketched in Fig. 1) fabricated on a standard 0.35 μm CMOS process. The devices

* Corresponding author.
E-mail address: sharma@iue.tuwien.ac.at (P. Sharma).

http://dx.doi.org/10.1016/j.microrel.2015.06.021
0026-2714/

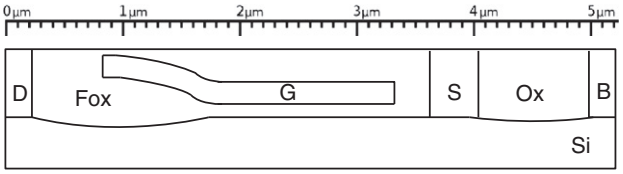

Fig. 1. Sketch of n-LDMOS transistor with all the segments marked: D — drain, S — source, Ox — oxide, Fox — field oxide, G — gate, B — bulk contact.

were stressed at the gate to source voltage $V_{gs} = 2$ V and drain to source voltages $V_{ds} = 18$ and 22 V at room temperature (300 K). The changes in the linear drain current ($\Delta I_{d,lin}$, obtained at $V_{ds} = 0.1$ V and $V_{gs} = 2.4$ V), saturation drain current ($\Delta I_{d,sat}$, obtained at $V_{ds} = 10$ V and $V_{gs} = 3.6$ V), and threshold voltages (ΔV_t) were monitored for stress times up to 1 Ms.

To obtain the device structure we used the Sentaurus process simulator [16], while for the device characteristics our device and circuit simulator MINIMOS-NT [17], used within the GTS framework [18], was employed. Both simulators were calibrated self-consistently to ensure reasonable agreement between the measured and evaluated characteristics of the fresh device. MINIMOS-NT uses the drift–diffusion simulation approach which is adequate for modeling the terminal currents in devices with longer channels [10]. It is important to emphasize that even in the case of the DD scheme, modeling of such a big device with a complicated geometry as the nLDMOS transistor is a non-trivial task. An important ingredient required for these simulations is a proper mesh. On the one hand, this mesh needs to be fine enough near the interface, at the bird's beak, and in other important device sections, while in less important segments (e.g. Si bulk) it can be coarser. On the other hand, it still has to contain a moderate number of mesh points to ensure fast and reliable convergence. To meet these requirements we used the adaptive meshing framework ViennaMesh which generates meshes based on the built-in potential [19,20].

3. The model

Our hot-carrier degradation model [4,3,21] employs the solution of the Boltzmann transport equation for the particular device topology and stress/operating conditions. The carrier distribution functions obtained are then used to simulate the interface state generation rates. In our model, HCD is attributed to breakage of the Si–H bonds at the Si/SiO_2 interface induced by the carrier ensemble. This ensemble contains both hot and colder carriers which can trigger single- and multiple-carrier processes of bond rupture [3]. In this context, the carrier DFs are needed to distinguish between the hotter and colder fraction of particles. In the model, we consider all possible superpositions of

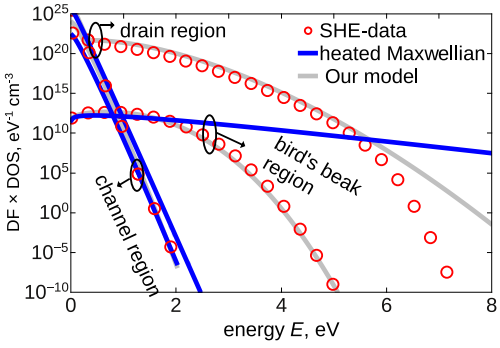

Fig. 2. The electron DFs (coupled with density of states to show the carrier occupancy) obtained with the heated Maxwellian approach compared with those simulated with ViennaSHE for $V_{gs} = 2$ V and for $V_{ds} = 18$ V calculated at the drain, bird's beak and channel regions. For comparison, the DFs evaluated with our DD-based model (light gray lines) are also plotted.

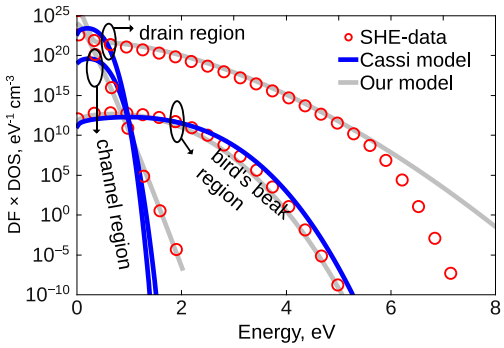

Fig. 3. Same as Fig. 2 but for the Cassi model.

these mechanisms [4,3]. Note that also in the case of long-channel and/or high-voltage devices, the multiple-carrier process has a significant contribution and cannot be ignored [22,3,14]. The interface state density profiles $N_{it}(x)$ are then evaluated for each stress time step and used in MINIMOS-NT to simulate the changes of the device characteristics over stress time. The effect of the defects generated during hot-carrier stress is twofold: they perturb the device electrostatics and scatter carriers, thereby degrading the carrier mobility.

A standard problem in HCD modeling is a possible contribution of oxide charges which were not considered here. There are two reasons for that. First, bulk oxide traps are known to be responsible for the recoverable component of degradation [23]. However, in our devices, no recovery was observed under the stress conditions used here. Second, our experience gained with the intimately related phenomenon of bias temperature instability suggests that trapping in the oxide bulk starts to play a prominent role at oxide fields of 6 MV/cm and higher [24]. The maximum oxide field in the nLDMOS transistors used was 1.3 MV/cm for $V_{ds} = 22$ V, $V_{gs} = 2$ V which is significantly smaller than 6 MV/cm. Therefore, the contribution of bulk oxide traps can be neglected.

Another important aspect which was also neglected in our model is the contribution of secondary holes generated by impact ionization [25]. The effect of holes is twofold: they can contribute to the interface trap generation and also be captured by existing amphoteric traps. The former mechanism was reported to be responsible for threshold voltage and drain current turn-around effects [26,27]. In our measurements we did not observe any turn-around effects, and thus we conclude that the hole contribution to HCD is weak. Drift-diffusion simulations performed for the nLDMOS device also showed that impact ionization leads to low or moderate hole concentrations throughout the channel.

Implementations of our HCD model vary in the particular method used to evaluate the carrier distribution function. We employ different approaches based on the results of the DD simulations. As a reference, we use the DFs (and the corresponding version of our HCD model) obtained by the direct solution of the BTE using ViennaSHE.

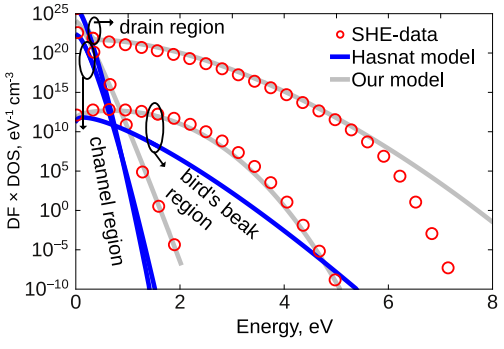

Fig. 4. Same as Fig. 2 but for the Hasnat model.

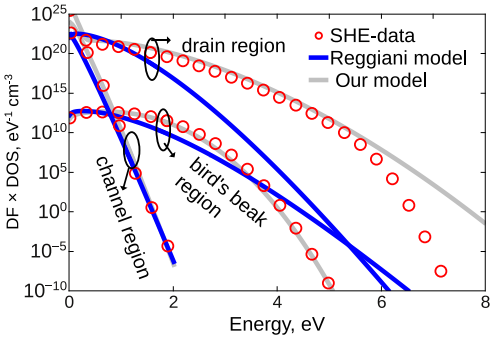

Fig. 5. Same as Fig. 2 but for the Reggiani model.

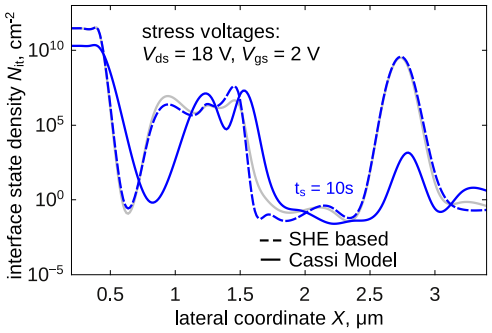

Fig. 7. Same as Fig. 6 but for the Cassi model.

The heated Maxwellian distribution is a frequently used approach to mimic the DFs of non-equilibrium carriers [10]:

$$f(\varepsilon) = A\exp(-\varepsilon/k_B T_n). \quad (1)$$

Here, k_B is the Boltzmann constant and T_n the carrier temperature which differs from the lattice temperature. An example of the DFs obtained using the Maxwellian function for different regions of the device is shown in Fig. 2. One can see that the DFs in the channel and drain regions are close to equilibrium, while in the bird's beak device section, the carriers are rather hot and the corresponding DFs are severely non-equilibrium.

Cassi and Riccó have proposed an expression to account for the non-Maxwellian shape of the DFs observed in the MOSFETs, especially in the drift and the drain regions. Their model for the DF is given by [11]

$$f(\varepsilon) = A exp\left(-\chi\varepsilon^3/E^{1.5}\right), \quad (2)$$

where $\chi = 0.1$ is a fitting parameter and E the local electric field. The Cassi model results in DFs which are substantially non-equilibrium in the bird's beak region, as shown in Fig. 3. Due to the fixed curvature, the shape of DF is similar in the channel and in the drain region. Hence, the carrier energies obtained from the Cassi model for these device sections are significantly lower as compared to the bird's beak region.

Hasnat et al. replaced the local electric field in Cassi's expression by a function of carrier temperature to capture the non-local behavior [12]:

$$f(\varepsilon) = A exp\left(-\varepsilon^{\xi}/(\eta(k_B T_n)^{\nu})\right), \quad (3)$$

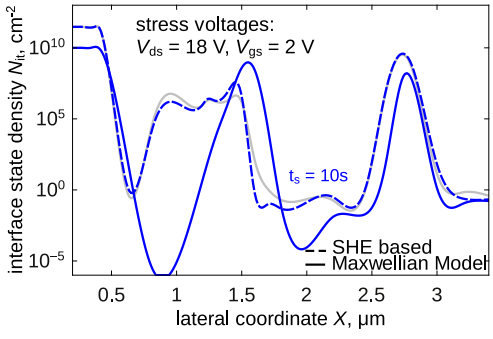

Fig. 6. The N_{it} profiles obtained using the heated Maxwellian (blue line), ViennaSHE (blue dashed line), and our DD-based approach (gray line) for $V_{gs} = 2$ V and for $V_{ds} = 18$ V and stress time of 10 s.

where ξ, η, and ν are fitting parameters. Fig. 4 shows the DFs obtained using Eq. (3) for different regions of the device. The DFs in the channel and the drain region are similar to the Maxwellian, see Fig. 2, while for the bird's beak region, the carrier energies obtained from the Hasnat model extend up to 5.5 eV and beyond.

Reggiani et al. have recently developed an analytical model for the DFs which is focused on modeling of HCD in LDMOS devices [28,29]. The DF is expressed as:

$$f(\varepsilon) = A\,exp[-\alpha\,\varepsilon(1+\delta\varepsilon)/(k_B T_n(1+\beta\varepsilon))]. \quad (4)$$

Here δ and β are fitting parameters, while A and α are evaluated using the carrier concentration n and carrier temperature T_n computed using the DD scheme. In long channel devices the moment n can be obtained directly from DD simulations while T_n is evaluated using the local energy balance equation [30]. The Reggiani model produces non-equilibrium DFs for the bird's beak and drain regions as shown in Fig. 5. As for the channel region, the corresponding DFs are close to the equilibrium ones.

Our HCD model is based on the approach suggested by our group previously in [31]:

$$f(\varepsilon) = A\exp\left(-(\varepsilon/\varepsilon_{ref})^b\right) + C\exp(-\varepsilon/k_B T_n). \quad (5)$$

The parameters in Eq. (5) are found using the available moment (n) of the Boltzmann transport equation, the carrier temperature (T_n) and the DF normalization [14]. The DFs obtained by our approach are shown in Figs. 2, 3, 4, and 5. One can see that our DD-based expression for the carrier distribution function can adequately represent the DF.

4. Results and discussion

To check the validity of the different HCD models we calculated the bond-breakage rates, the interface state density profiles, and then the

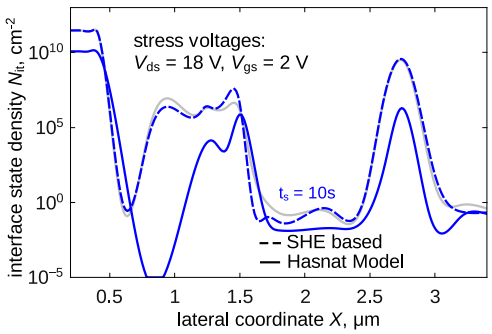

Fig. 8. Same as Fig. 6 but for the Hasnat model.

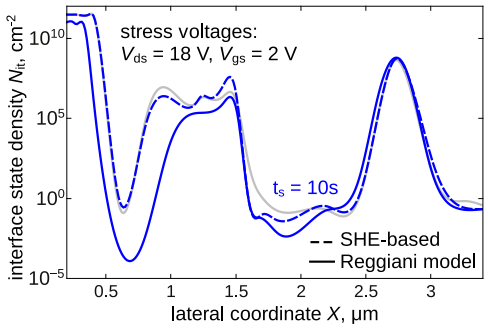

Fig. 9. Same as Fig. 6 but for the Reggiani model.

change of the linear and saturation drain currents ($\Delta I_{d,lin}$, $\Delta I_{d,sat}$) as well as the threshold voltage shift (ΔV_t). The data obtained from the different versions of the model are compared against the HCD results measured in nLDMOS transistors.

4.1. Distribution functions and interface state densities

The heated Maxwellian DFs are compared to those calculated with ViennaSHE in Fig. 2. As expected, the Maxwellian model is only valid in the channel region where the carriers are almost in equilibrium. It overestimates the DFs at high energies in the bird's beak and fails completely in the drain region of the nLDMOS device. The heated Maxwellian distribution leads to reasonable $N_{it}(x)$ profiles only in the channel and source regions when compared with the $N_{it}(x)$ profiles computed using the DF from ViennaSHE, see Fig. 6. This approach overestimates the N_{it} values in the bird's beak region and also fails in the drain section.

The *Cassi model* shows an improvement for the non-equilibrium case but cannot describe the DFs near the drain. This is because the DFs evaluated with this approach have a fixed curvature. Fig. 7 summarizes the $N_{it}(x)$ profiles obtained using the DFs from the Cassi model and from ViennaSHE. These $N_{it}(x)$ profiles from the two approaches are only comparable in the bird's beak region. Such a behavior is also consistent with the difference in the DFs computed with this model and that using the exact BTE solution.

The *Hasnat model* cannot represent the DFs in either the bird's beak or the drain region, as shown in Fig. 4. The corresponding interface trap density is plotted in Fig. 8, which do not match those calculated with ViennaSHE in the entire x coordinate range. The N_{it} values are severely underestimated inside the channel and close to the drain region.

The *Reggiani model* appears promising because it can describe the DFs in LDMOS devices with good accuracy except for the drain region. The reason is that within the Reggiani model the DFs are linked to the local electric field, and thus hot carriers which form the high-energy tail of the DF are not properly described. From Fig. 5 one can see that the high-energy tails of the DF are underpopulated if the Reggiani model is used. As a result, this discrepancy translates also to an error in N_{it} which is underestimated in the drain, as is evident from Fig. 9.

Figs. 2, 3, 4, and 5 also show the DFs computed with our model (light gray curves) which was successful in representing the carrier distribution along the entire device. A discrepancy appears in the drain region for energies higher than ~6 eV where the DF values have already dropped by more than 20 orders of magnitude. Thus, this discrepancy does not translate into an error in the calculated HCD, see [32,14]. The N_{it} density simulated by our DD-based model is quite accurate, thereby suggesting that a slight discrepancy observed in the drain DFs at ~6 eV does not affect the $N_{it}(x)$ profiles.

4.2. Degradation traces

The changes in $I_{d,lin}(t)$, $I_{d,sat}(t)$, and $V_t(t)$ calculated with the different model versions are summarized and compared to the experimental data in Figs. 10, 11, 12, and 13.

The *heated Maxwellian approach* leads to a saturation of $\Delta I_{d,lin}(t)$, $\Delta I_{d,sat}(t)$, and $\Delta V_t(t)$ at ~500 s, see Fig. 10. Such a behavior is related to

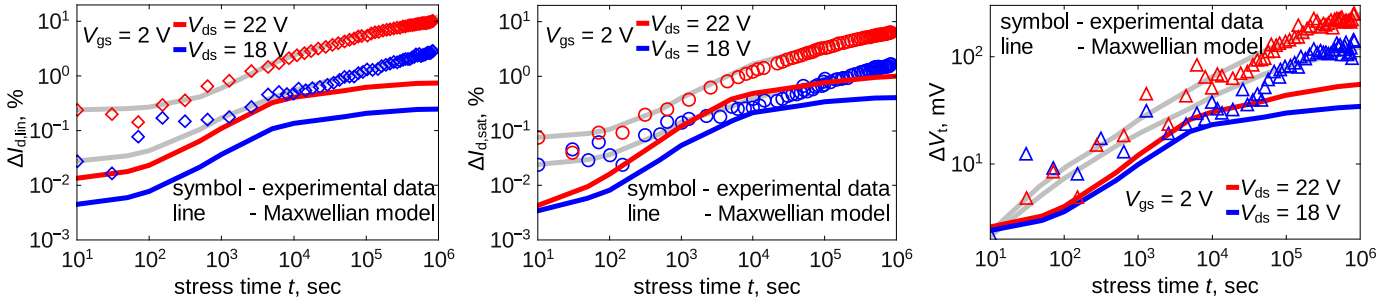

Fig. 10. Simulated $\Delta I_{d,lin}(t)$, $\Delta I_{d,sat}(t)$ and $\Delta V_t(t)$ traces obtained using the heated Maxwellian against experimental data. Stress voltages are $V_{gs} = 2$ V and $V_{ds} = 18$ and 22 V. As a reference, the degradation traces obtained with our DD-based version of the model are plotted (gray curves).

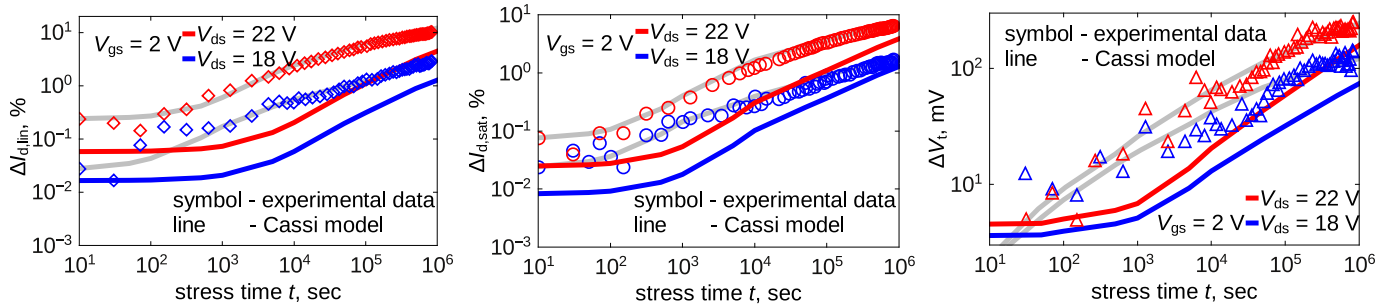

Fig. 11. Same as Fig. 9 but for the Cassi model.

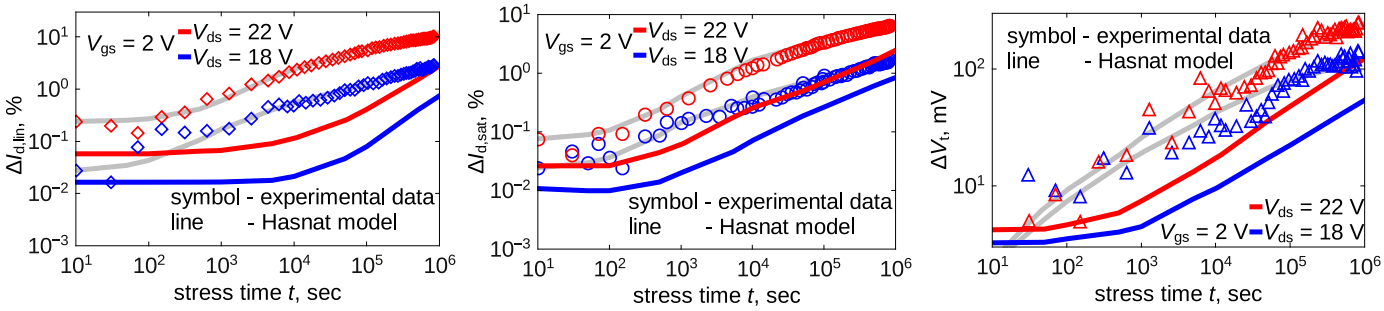

Fig. 12. Same as Fig. 9 but for the Hasnat model.

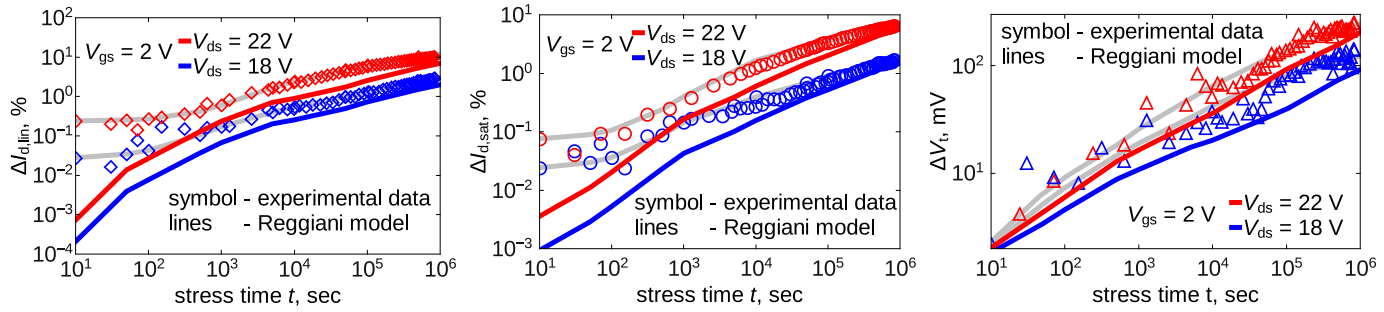

Fig. 13. Same as Fig. 9 but for the Reggiani model.

the drain N_{it} peak which is formed by hot carriers and which determines short term hot-carrier degradation [22,14,32]. One can see that the interface state density N_{it} is saturated already at short stress times, and thus at long stress times, HCD is driven by colder carriers which contribute to the multiple-carrier process [22,14,32]. As a result, if the effect of cold carriers is underestimated, the change of the device characteristics saturates at longer stress times.

Figs. 3 and 7 show that the *Cassi model* highly underestimates the DFs and N_{it} values near the drain region. As a consequence, the degradation of all device characteristics is underestimated as well, especially at short stress times. This is because the most prominent discrepancy between the DFs obtained with ViennaSHE and the Cassi model is visible for the drain section of the device. The same behavior is typical also for the N_{it} drain maximum, which – as we already discussed – determines short-term HCD.

The *Hasnat model* behaves similarly to the Cassi model where the DF values are underestimated for most of the device regions. As a result, the degradation of both saturation and drain currents as well as the threshold voltage shift are massively underestimated in the entire experimental stress time window, see Fig. 12.

As for the *Reggiani model*, as we already discussed, the model underestimates the interface trap density near the drain. This peculiarity results in a weaker curvatures of $\Delta I_{d,sat}(t)$, $\Delta I_{d,lin}(t)$, and $\Delta V_t(t)$ traces as shown in Fig. 13. Although the degradation curves are close to the experimental ones at long stress times, they are unable to predict the correct degradation for the entire stress time slot.

Finally, Figs. 10, 11, 12, and 13 show very good agreement between measured $\Delta I_{d,lin}(t)$, $\Delta I_{d,sat}(t)$, and $\Delta V_t(t)$ curves and those simulated with our DD-based HCD model for the whole stress time window. It is important to emphasize that both SHE- and DD-based versions of our model use the same set of the model parameters for different combinations of stress voltages and for the degradation traces of different device characteristics.

5. Conclusions

Using hot-carrier degradation data measured on nLDMOS devices, we have performed a comparison between various HCD models which employ different approaches to solve or approximate the Boltzmann transport equation. In several realizations of our HCD model we used carrier energy distribution functions obtained with the heated Maxwellian, Cassi, Hasnat, Reggiani and our own model. We have compared these different versions in terms of carrier DFs, interface state density profiles, and degradation of the linear and saturation drain currents, as well as the threshold voltage. The heated Maxwellian neglects the cold carrier fraction of the carrier ensemble and thus the N_{it} profiles are adequate to some extend only in the channel and source regions. As a result, the degradation traces ($\Delta I_{d,lin}(t)$, $\Delta I_{d,sat}(t)$, and $\Delta V_t(t)$) show a spurious saturation at longer stress times. The Cassi and Hasnat models underestimate the values of the carrier DFs in most of the device regions. As for the N_{it} profiles, the former approach leads to somewhat reasonable N_{it} values only near the bird's beak, while the interface state densities simulated with the latter approach have substantially lower values (as compared to those evaluated using the BTE solution) in the entire range of the lateral coordinate. Therefore, the $\Delta I_{d,lin}(t)$, $\Delta I_{d,sat}(t)$ and $\Delta V_t(t)$ degradation characteristics computed using the Cassi and Hasnat models are underestimated within the entire stress time slot. The Reggiani model can represent the DFs for most device regions except the drain where the agreement deteriorates. As a result, the curvature of the degradation traces is weaker within the Reggiani model. Finally, our DD-based method can mimic the DFs in the entire device with a slight discrepancy in the drain region for the high energy tails where the magnitude of DF has already dropped by ~20 orders. This discrepancy does not translate to an error in the results evaluated using this approach. This means that the agreement between the $N_{it}(x)$ profiles and the $\Delta I_{d,lin}(t)$, $\Delta I_{d,sat}(t)$, and $\Delta V_t(t)$ degradation curves simulated with the SHE- and DD-based realization of the model is very

good. We, therefore, conclude that in long-channel LDMOS transistors HCD can be modeled with very good accuracy even with a DD-based formalism provided a better approximative model for the distribution function is used.

Acknowledgments

The authors acknowledge support by the Austrian Science Fund (FWF, grants P23598 and P26382), by the European Union FP7 project ATHENIS_3D (grant No 619246) and by the European Research Council (ERC) project MOSILSPIN (grant No 247056).

References

[1] W. McMahon, K. Matsuda, J. Lee, K. Hess, J. Lyding, The effects of a multiple carrier model of interface states generation of lifetime extraction for MOSFETs, *Proc. Int. Conf. Mod. Simul. Microsys*, vol. 1 2002, pp. 576–579.
[2] S. Reggiani, S. Poli, M. Denison, E. Gnani, A. Gnudi, G. Baccarani, S. Pendharkar, R. Wise, Physics-based analytical model for HCS degradation in STI-LDMOS transistors, IEEE Trans. Electron Dev. 58 (2011) 3072–3080.
[3] S. Tyaginov, M. Bina, J. Franco, D. Osintsev, O. Triebl, B. Kaczer, T. Grasser, Physical modeling of hot-carrier degradation for short- and long-channel MOSFETs, Proc. International Reliability Physics Symposium (IRPS) 2014, pp. 1–8.
[4] M. Bina, S. Tyaginov, J. Franco, Y. Wimmer, D. Osinstev, B. Kaczer, T. Grasser, Predictive hot-carrier modeling of N-channel MOSFETs, IEEE Trans. Electron Dev. 61 (9) (2014) 3103–3110.
[5] A. Bravaix, C. Guerin, V. Huard, D. Roy, J.-M. Roux, E. Vincent, Hot-carrier acceleration factors for low power management in DC–AC stressed 40 nm NMOS node at high temperature, Proc. International Reliability Physics Symposium (IRPS) 2009, pp. 531–546.
[6] S. Tyaginov, T. Grasser, Modeling of hot-carrier degradation: physics and controversial issues, Proc. International Integrated Reliability Workshop (IIRW) 2012, pp. 206–215.
[7] C. Jungemann, B. Meinerzhagen, *Hierarchical device simulation*. 1 em plus 0.5 em minus 0.4 em, Springer Verlag, Wien/New York, 2003.
[8] M. Fischetti, S. Laux, Monte-Carlo study of sub-band-gap impact ionization in small silicon field-effect transistors, Proc. International Electron Devices Meeting (IEDM) 1995, pp. 305–308.
[9] S.-M. Hong, A. Pham, C. Jungemann, *Deterministic solvers for the Boltzmann transport equation*. 1 em plus 0.5 em minus 0.4 em, Springer, 2011.
[10] T. Grasser, T.-W. Tang, H. Kosina, S. Selberherr, A review of hydrodynamic and energy-transport models for semiconductor device simulation, Proc. IEEE 91 (2) (2003) 251–273.
[11] D. Cassi, B. Ricco, An analytical model of the energy distribution of hot electrons, IEEE Trans. Electron Dev. 37 (6) (1990) 1514–1521.
[12] K. Hasnat, C.-F. Yeap, S. Jallepalli, S.A. Hareland, W.-K. Shih, V.M. Agostinelli, A.F. Tasch, C.M. Maziar, Thermionic emission model of electron gate current in submicron NMOSFETs, IEEE Trans. Electron Dev. 44 (1) (1997) 129–138.
[13] S. Reggiani, G. Barone, E. Gnani, A. Gnudi, G. Baccarani, S. Poli, R. Wise, M.-Y. Chuang, W. Tian, S. Pendharkar, M. Denison, Characterization and modeling of electrical stress degradation in STI-based integrated power devices, Solid-State Electron. 102 (12) (2014) 25–41.
[14] P. Sharma, S. Tyaginov, Y. Wimmer, F. Rudolf, K. Rupp, M. Bina, H. Enichlmair, J.-M. Park, R. Minixhofer, H. Ceric, T. Grasser, Modeling of hot-carrier degradation in nLDMOS devices: different approaches to the solution of the Boltzmann transport equation, IEEE Trans. Electron Devices. 62 (6) (2015) 1–8.
[15] ViennaSHE, http://viennashe.sourceforge.net/.
[16] *Synopsys, Sentaurus Process, Advanced Simulator for Process Technologies*.
[17] *MINIMOS-NT Device and Circuit Simulator*, Institute for Microelectronic, TU Wien.
[18] http://www.globaltcad.com/en/products/minimos-nt.html.
[19] ViennaMesh, http://viennamesh.sourceforge.net/.
[20] F. Rudolf, K. Rupp, J. Weinbub, A. Morhamer, and S. Selberherr, "Transformation Invariant Local Element Size Specification", Journ. Appl. Math. Camput., in press.
[21] S. Tyaginov, M. Bina, J. Franco, Y. Wimmer, D. Osintsev, B. Kaczer, T. Grasser, A predictive physical model for hot-carrier degradation in ultra-scaled MOSFETs, Proc. Simulation of Semiconductor Processes and Devices (SISPAD)2014. 89–92.
[22] Y. Wimmer, S. Tyaginov, F. Rudolf, K. Rupp, M. Bina, H. Enichlmair, J.-M. Park, R. Minixhofer, T. Grasser, Physical modeling of hot-carrier degradation in nLDMOS transistors, Proc. International Integrated Reliability Workshop (IIRW), 2014 (in press).
[23] T. Grasser, "Stochastic Charge Trapping in Oxides: From Random Telegraph Noise to Bias Temperature Instabilities", Microelectronics Reliability (invited), vol. 52, no. 1, pp. 39–70.
[24] D. Schroder, J. Babcock, Negative bias temperature instability: road to cross in deep submicron silicon semiconductor manufacturing, J. Appl. Phys. 94 (1) (2003) 1–18.
[25] S. Tyaginov, I. Starkov, O. Triebl, H. Enichlmair, C. Jungemann, J. Park, H. Ceric, T. Grasser, Secondary generated holes as a crucial component for modeling of HC degradation in high-voltage n-MOSFET, *Proc. International Conference on Simulation of Semiconductor Processes and Devices (SISPAD)* 2011, pp. 123–126.
[26] J.F. Chen, S.-Y. Chen, K.-M. Wu, C.M. Liu, "Investigation of hot-carrier-induced degradation mechanisms in p-type high-voltage drain extended metal-oxide-semiconductor transistors", Japan J. Appl. Phys. 48 (4S) (2009).
[27] I. Starkov, H. Enichlmair, S.E. Tyaginov, T. Grasser, Analysis of the threshold voltage turn-around effect in high-voltage n-MOSFETs due to hot-carrier stress, Proc. IRPS 2012, pp. XT.7.1–XT.7.6.
[28] S. Reggiani, G. Barone, S. Poli, E. Gnani, A. Gnudi, G. Baccarani, M.-Y. Chuang, W. Tian, R. Wise, TCAD simulation of hot-carrier and thermal degradation in STI-LDMOS transistors, IEEE Trans. Electron Devices 60 (2) (2013) 691–698.
[29] S. Reggiani, G. Barone, E. Gnani, A. Gnudi, G. Baccarani, S. Poli, M.-Y. Chuang, W. Tian, R. Wise, TCAD predictions of linear and saturation HCS degradation in STI-based LDMOS transistors stressed in the impact-ionization regime, Proc. ISPSD (2013) 375–378.
[30] T. Grasser, H. Kosina, C. Heitzinger, S. Selberherr, Characterization of the hot electron distribution function using six moments, J. Appl. Phys. 91 (6) (2002) 3869–3879.
[31] T. Grasser, H. Kosina, C. Heitzinger, S. Selberherr, Accurate impact ionization model which accounts for hot and cold carrier populations, Appl. Phys. Lett. 80 (4) (2002) 613–615.
[32] P. Sharma, S. Tyaginov, Y. Wimmer, F. Rudolf, H. Enichlmair, J.-M. Park, H. Ceric, T. Grasser, A model for hot-carrier degradation in nLDMOS transistors based on the exact solution of the Boltzmann transport equation versus the drift-diffusion scheme, *Proc. EUROSOI-ULIS* 2015, pp. 21–24.